Critical role of flow-modified permittivity in electrorheology: Model and computer simulation

Ujitha M. Dassanayake
Complex Fluids Group, Physics Department, Brandeis University, Waltham, Massachusetts 02454, USA

Stella S. R. Offner and Yue Hu
Physics Department, Wellesley College, Wellesley, Massachusetts 02481, USA

(Received 18 November 2003; published 27 February 2004)

We propose a model that takes into account the effect of flow-modified permittivity (FMP) on electrorheology (ER). Our computer simulation shows that for Mason numbers less than 0.1, ER effects are mainly attributable to the deformation of chain structures, in agreement with earlier theoretical and simulation work. At larger Mason numbers, where chain structures have been destroyed by shear flows, we show that an FMP-induced misalignment between the particle dipole moments and the applied electric field plays a crucial role in producing ER effects. We also identify conditions under which negative ER effects are seen at large Mason numbers.

DOI: 10.1103/PhysRevE.69.021507 PACS number(s): 83.10.−y, 83.50.Ax, 83.60.Np, 83.80.Gv

I. INTRODUCTION

Electrorheological (ER) fluids are suspensions of small particles (0.1–100 μm) in insulating fluids. When an external electric field on the order of 1 kV/mm is applied to an ER fluid, the viscosity of the fluid increases dramatically. The ER response time is fast (on the order of milliseconds), and the effect is reversible. Since it was first discovered by Winslow in the 1940s [1], electrorheology has attracted the attention of scientists in both academia and industry. ER fluids could potentially revolutionize electrically controlled stress-transfer systems, such as active dampers, hydraulic valves, clutches, brakes, and actuators [2]. Despite their promise, however, commercially viable ER devices have not become widely available due to an absence of high-quality ER fluids. Many scientists believe that a fundamental understanding of the mechanism responsible for ER effects is needed in order to improve ER fluids. Unfortunately, such an understanding has been lacking [3].

In the absence of an external electric field, ER fluids generally behave like Newtonian fluids with the shear stress τ proportional to the shear rate $\dot{\gamma}$. This proportionality constant is the viscosity of the fluid η. When an external E field is applied to an ER fluid in a direction perpendicular to the shear flow, the fluid shows Bingham behavior [Eq. (1)]. The E field produces an increment in the shear stress (τ_E) that remains nearly constant over a large range of shear rates, giving rise to an apparent yield stress. The following equation is commonly used to describe ER effects:

$$\tau = \tau_E + \eta_0 \dot{\gamma}, \tag{1}$$

where η_0 is the viscosity of the fluid in the absence of an E field. The onset of flow in ER fluids is generally complex, and it is not known whether ER fluids have a true static yield stress [2]. It has been observed that the shear stress in ER fluids can decrease sharply following the onset of flow but still remain larger than the zero-E-field values. When the shear rate is reduced to zero from nonzero values, the shear stress shows hysteresis, and the apparent yield stress is less than the value obtained at the onset of flow [2].

It has been known since Maxwell's time that when an external E field is applied to a suspension of small particles, the particles become polarized. For ER fluids, the interactions between the polarized particles cause the particles to line up in the direction of the applied field, forming chains and columns that span the gap between the electrodes when the fluids are quiescent. Traditionally, ER effects have been attributed to the additional stress needed to break up these chains and column structures [4,5]. (This is called the chain model.)

The dimensionless quantity that characterizes the relative importance of the hydrodynamic forces on a particle compared to the electrostatic forces between particles is the Mason number $\mathrm{Mn} = \eta\dot{\gamma}/2\varepsilon_0\varepsilon_f\beta_0^2E_a^2$, where η and ε_f are the viscosity and the dielectric constant of the suspending fluid, respectively, ε_0 is the permittivity of the vacuum, β_0 is the Clausius-Mossotti factor, and E_a denotes the applied field strength. When the Mason number is small, hydrodynamic forces are not sufficient to easily break up the chain structures in an ER fluid, and this results in strong ER effects. ER effects, however, diminish as the Mason number increases. Some model ER fluids show no ER effects for $\mathrm{Mn} > 1$ [6].

The chain model has been successful in predicting the yield stress [7,8] and in determining the microstructure of model ER fluids with uniform particles and no flow [9]. Computer simulation work has shown that the chains are critical for ER effects and that the E-field-induced shear stress goes to zero if the chain structures are destroyed by a shear flow, as happens for Mason numbers larger than 0.1 [10]. Critics of the chain model, on the other hand, have argued that when ER fluids undergo a shear flow, the measured ER effects are still appreciable, even when the chain structures are not maintained [2,11]. For example, some ER fluids show ER effects at Mason numbers above 10 [12,13].

In most ER measurements, dc electric fields are used. Under dc conditions, the degree of polarization of particles suspended in a fluid is determined by the conductive properties of the particles and of the fluid [14]. A conduction model has

been proposed [15] which takes into account the distortion of electric field lines within the small gaps between particles. Critics of the conduction model, however, point out that the conduction model is static and does not consider the dynamic processes of an ER fluid in a shear flow [16]. In addition, attempts to develop ER fluids using metal particles with insulator coatings have been unsuccessful [17].

It is puzzling why maximizing dielectric or conductive mismatch between particles and fluids fails to produce good ER fluids, even though maximum particle polarization is obtained under these conditions. Experimentally, ER effects do not seem to be particularly sensitive to the details of the particle polarization mechanism, and many different kinds of particles—ionic conductors, semiconductors, and insulating particles with conducting surface layers—have shown ER effects [11]. A common feature among many different kinds of ER fluids seems to be an optimal dielectric relaxation frequency that generally falls within the range of 10^2–10^5 Hz [2].

It is not difficult to understand that there should be a lower limit for the optimal dielectric relaxation rate. In a shear flow of shear rate $\dot{\gamma}$, a spherical particle spins at an angular velocity $\Omega = \dot{\gamma}/2$ [18]. The effect of this spinning motion on particle polarization has been carefully studied, both experimentally [19,20] and theoretically [21–23]. In general, the magnitude of the particle dipole moment decreases as the particle spinning rate increases, because the particle spinning motion interferes with the migration of mobile charge carriers in the particle in response to the applied electric field. There is, however, a resonance peak in the dielectric constant as a function of shear rate and as a function of electric field frequency when the particle spinning rate and the angular frequency of the applied field exactly match. This flow-modified permittivity (FMP) and the resonance peaks can be used to monitor the particle spinning rate.

The existence of an upper limit for the optimal dielectric relaxation rate, however, is difficult to justify using the chain model, since the polarization of a particle with a high dielectric relaxation rate is not appreciably affected by the spinning motion of the particle. A single-particle model for ER effects has been proposed [18]. In this model, the spin of a particle in a shear flow induces a dipole moment misaligned with the applied electric field, and this results in an electric torque on the particle. The electric torque retards and possibly even halts the spinning motion of the particle and hence creates additional dissipation. (This is the locking model.) This model was examined experimentally by measuring FMP while applying a large dc field [24]. The particle spinning rate, however, showed no detectable shift from the free-particle value in dc fields up to 1 kV/mm, thus demonstrating that the locking effect was not the main factor contributing to ER effects. Another experiment revealed a slight reduction in the particle spinning rate at field strengths greater than 1 kV/mm, although the particles never completely stopped spinning in fields as strong as 4 kV/mm [25].

Computer simulations of ER effects have generally been carried out in the limit of dipole-dipole interactions [26–29].

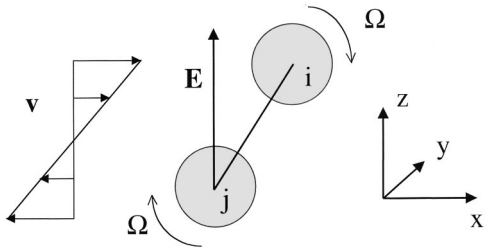

FIG. 1. Two particles in a shear flow. The applied electric field is in the *z* direction. The shear flow induces particles to spin about the *y* axis with an angular velocity $\Omega = \dot{\gamma}/2$.

Some simulations have included mutual polarization between particles [5,10,30], but to the best of our knowledge, FMP has not been considered for interparticle interactions. In this paper, we propose a model for ER effects in which FMP is taken into account. In particular, we use the results of previous theoretical studies of single-particle FMP to examine the effects of FMP on interactions between particles and on the rheological properties of ER fluids. For small Mason numbers, we show that our model is consistent with the chain model. At larger Mason numbers—where previous theoretical studies have shown no ER effect—we obtain ER effects, even in the absence of chain structures. In addition, we see negative ER effects under certain conditions, providing theoretical support for previously unexplained experimental observations [31,32]. A preliminary computer simulation based on this model is also reported here.

II. MODEL AND SIMULATION

We consider the simple case of a particle of radius R immersed in a fluid. The dielectric constants and conductivities of the particle and of the fluid are ε_p, σ_p and ε_f, σ_f, respectively [33]. The dipole moment induced by an applied E field can be described by Maxwell-Wagner polarization with a Debye-type relaxation time $\tau_{MW} = \varepsilon_0(\varepsilon_p + 2\varepsilon_f)/(\sigma_p + 2\sigma_f)$ [14].

If a shear flow of shear rate $\dot{\gamma}$ is imposed on a fluid, a particle suspended in the fluid undergoes a spinning motion with an angular velocity $\Omega = \dot{\gamma}/2$. This spinning motion affects the motion of charge carriers in the particle. For example, charge carriers (assumed positive) in particle *i* in Fig. 1 move upward in response to the applied E field. Because of the particle spinning motion, charge carriers on the left side move faster than the charge carriers on the right side, resulting in an equilibrium charge distribution that is not symmetric with respect to the E field. In general, the shear flow induces a complex particle dipole moment in directions both parallel and perpendicular to the applied electric field.

In an E field of magnitude E_a and angular frequency ω, the dipole moment for a particle with a Debye-type relaxation is [21]

$$\vec{\mu} = 4\pi\varepsilon_0\varepsilon_f R^3 E_a e^{i\omega t}\vec{\alpha}, \tag{2}$$

where the components of $\vec{\alpha}$ in directions parallel and perpendicular to the applied field are:

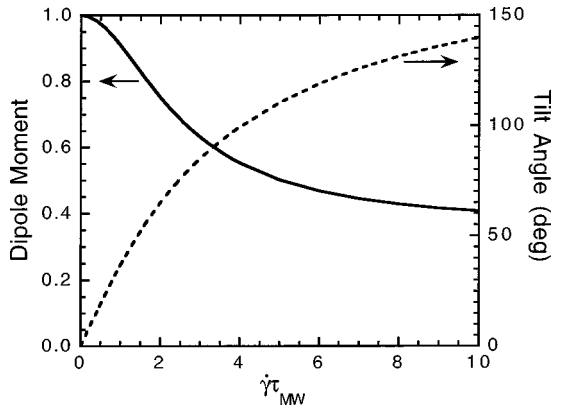

FIG. 2. The direction (tilt angle) and magnitude of the induced particle dipole moment as a function of shear rate normalized by the Maxwell-Wagner relaxation frequency. The applied field is dc and is in the z direction. We choose $\varepsilon_f/\varepsilon_p=5$ and $\sigma_f=0$.

$$\alpha_{\parallel}=\beta_{\infty}+(\beta_0-\beta_{\infty})\frac{1+i\omega\tau_{MW}}{1-(\omega^2-\Omega^2)\tau_{MW}^2+2i\omega\tau_{MW}}, \quad (3)$$

$$\alpha_{\perp}=(\beta_0-\beta_{\infty})\frac{\Omega\tau_{MW}}{1-(\omega^2-\Omega^2)\tau_{MW}^2+2i\omega\tau_{MW}}. \quad (4)$$

Here β_0 and β_{∞} are the low- and high-frequency limits of the Clausius-Mossotti factor: $\beta_0=(\sigma_p-\sigma_f)/(\sigma_p+2\sigma_f)$ and $\beta_{\infty}=(\varepsilon_p-\varepsilon_f)/(\varepsilon_p+2\varepsilon_f)$.

In this paper, we limit our discussion to dc fields ($\omega=0$). Furthermore, we assume $\sigma_f=0$, because in most ER fluids the particles are much more conductive than the fluid. Figure 2 shows the direction and the magnitude of the dimensionless dipole moment $\vec{\alpha}$ calculated as a function of $\dot{\gamma}\tau_{MW}$ for $\varepsilon_f/\varepsilon_p=5$ using Eqs. (3) and (4). In the absence of shear, the dipole moment points in the same direction as the applied E field, and the magnitude of the dipole moment is determined by the conductive mismatch between the particle and the fluid (maximal mismatch here because $\sigma_f=0$). In the presence of shear, the dipole moment tilts in the direction of the flow. At high shear rates, the magnitude of the dipole moment is determined by the dielectric mismatch between the particle and the fluid.

In a suspension of many particles, the motion of each particle is determined by hydrodynamic forces, electric interactions ($\vec{F}_{ele}$), and hard-core repulsive forces ($\vec{F}_{rep}$). For simplicity, we ignore the hydrodynamic interactions between the particles and consider only Stokes forces. In the limit of overdamped motion, the acceleration of the particles can be neglected, and the net force on each particle is zero at any given moment [26]. For computational convenience, we introduce the following scaling factors for force, length, and time: $F_0=3\pi\varepsilon_0\varepsilon_f\beta_0^2\overline{R}^2E_a^2/4$, $l_0=2\overline{R}$, and $t_0=3\pi\eta l_0^2/F_0$, where $\overline{R}$ is the mean particle radius and η is the viscosity of the suspending fluid. In dimensionless units, the equation of motion for particle i (with diameter d_i^* and z coordinate z_i^*) in Fig. 1 is [26]

$$\frac{d\vec{r}_i^*}{dt^*}=\vec{v}_f^*(\vec{r}_i^*)+\frac{1}{d_i^*}(\vec{F}_{ele}^*+\vec{F}_{rep}^*), \quad (5)$$

where we have used asterisks to denote dimensionless quantities and where $\vec{v}_f^*(\vec{r}_i^*)=\dot{\gamma}^*z_i^*\hat{x}$ is the shear field. We also point out that our dimensionless shear rate $\dot{\gamma}^*$ is proportional to the Mason number. ($\dot{\gamma}^*=32$ Mn here.)

The electric forces between particles are assumed to arise mainly from dipole-dipole interactions, and we ignore multipole moments and mutual polarization. In Fig. 1, the electric force exerted by particle j on particle i is

$$\vec{F}_{ele,ji}^*=(\vec{\alpha}\cdot\nabla)\frac{d_i^{*3}d_j^{*3}}{3r_{ji}^{*3}}[3\hat{r}_{ji}(\vec{\alpha}\cdot\hat{r}_{ji})-\vec{\alpha}], \quad (6)$$

where $\hat{r}_{ji}$ is the unit vector pointing from the center of particle j to the center of particle i, and the components of $\vec{\alpha}$ are given by Eqs. (3) and (4) with $\omega=0$ and $\beta_0=1$.

To prevent particle overlapping, we adopt a hard-core repulsive force similar to the one used by Klingenberg and co-workers [26]. The repulsive force exerted by particle j on particle i in Fig. 1 is

$$\vec{F}_{rep,ji}^*=a\exp\left[\frac{(d_i^*+d_j^*)/2-|\vec{r}_i^*-\vec{r}_j^*|}{b}\right]\hat{r}_{ji}, \quad (7)$$

where $a=2$ and $b=0.01$ are constants and the repulsive force is along the line connecting the centers of the two particles.

The shear stress can be calculated using the equation [34]

$$\tau_{xz}^*=-\frac{1}{V^*}\sum_{i=1}^{N}f_{x,i}^*z_i^*, \quad (8)$$

where V^* is the system volume, $f_{x,i}^*$ is the x component of the net electric force and hard-core repulsion on particle i, z_i^* is the z coordinate of particle i, and the sum is over all N particles.

III. SIMULATION RESULTS

The simulation is carried out using an Euler method with shifted periodic boundary conditions. For each simulation, 250 particles are initially placed in an $8\times8\times8$ box, and the positions of the particles are updated with a fixed time step of $\Delta t^*=2\times10^{-5}$. The particle radii have a mean value of 0.50 and a standard deviation of 0.14. The particle volume fraction is 0.32. The shear stress is obtained by averaging a total of 1×10^6 steps and by averaging over two different initial configurations.

We first discuss particle configurations during a shear flow when an electric field is applied. For clarity, we present the results of a two-dimensional simulation [35]. Figure 3(a) shows an initial configuration. Figure 3(b) shows one snapshot of the particle distribution while the system is being sheared at Mn=0.03. We can see particle chain structures stretched by the shear flow. At a higher Mason number of 3

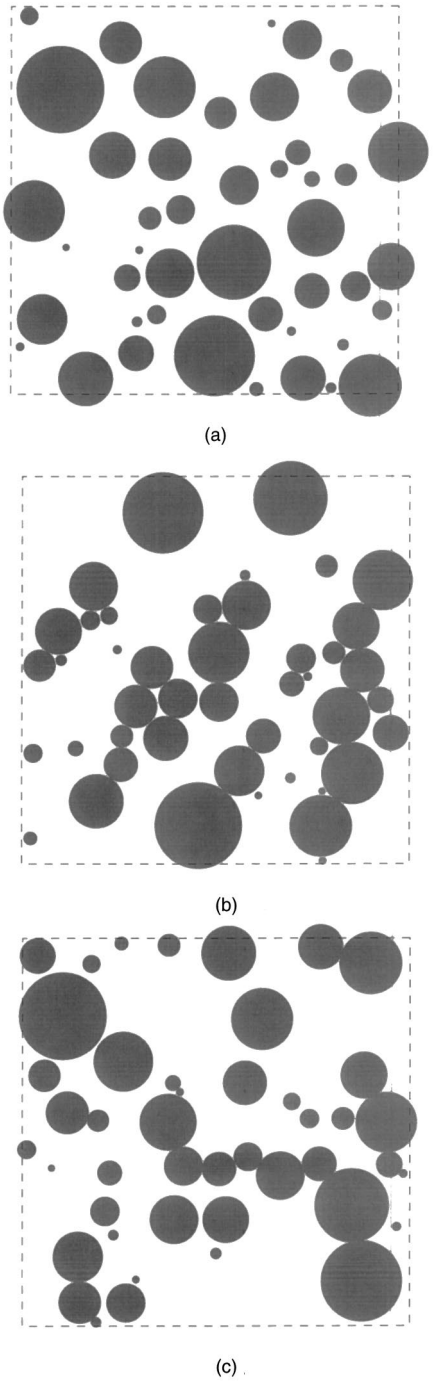

FIG. 3. (a) A typical initial configuration with 45 particles randomly placed in a 12×12 box. (b) Particle configuration at Mn $=0.03$. Chain structures are tilted in the direction of the flow. (c) Particle configuration at Mn$=3$. Particles do not form chains at this large Mason number.

[Fig. 3(c)], however, the chain structures no longer exist. This change in structure with shear rate can be understood in terms of the competing effects of electric interactions and viscous drag: The electric interactions act to align the particles in chains, while the shear drag tries to break them apart. In this paper we call the region in which chain structures exist ''low shear'' and the region with no chain structures ''high shear.''

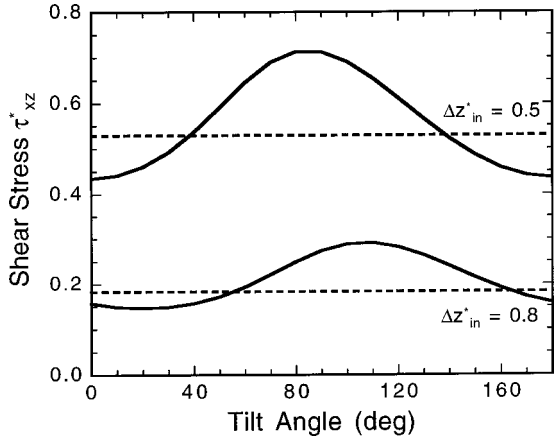

FIG. 4. Average shear stress for two identical particles colliding with each other as a function of dipole tilt angle. The Mason number is one, and the initial z separations between the particles are 0.5 and 0.8. The dotted lines are the shear stresses without the electric forces.

The transition point between the low shear and high shear regions can be roughly estimated by considering the following situation. Two identical particles of diameter 1 are polarized along the direction of the electric field ($\alpha_{\parallel}=1$ and $\alpha_{\perp}=0$) and are initially aligned in the direction of the applied field with a center-to-center separation of $r^*=1$. Our simulation shows that it takes a shear flow of Mn$\geqslant0.1$ to pull these two particles apart, and so we consequently estimate the critical Mason number to be $\mathrm{Mn}_c\simeq0.1$. This transition point is close to the experimentally observed value of Mn $=0.3$ for the onset of shear thinning [36].

To investigate whether it is possible to obtain ER effects in the high shear region, we first examine a situation in which only two particles of diameter 1 encounter each other in a shear flow of Mn$=1$. The initial and final separation between the particles in the direction parallel to the flow is $|\Delta x^*|=3$. Two initial z separations are used: $\Delta z^*=0.5$ and 0.8. The magnitude of the dipole moment is set to 1, and only the dipole tilt angle is varied. Figure 4 shows the average shear stress for different dipole tilt angles, and these results are compared with results obtained when the electric interactions are set to zero. (When the electric interactions are set to zero, the horizontal axis should be converted to shear rate using the electric field strength *before* it is set to zero.) We can clearly see that the tilt angle plays an important role in producing ER effects. If the tilt angle is zero (i.e., if the dipole moment is parallel to the applied field), a *negative* ER effect is obtained. A positive ER effect is achieved only when the tilt angle falls within the middle range of the graph.

From Fig. 4 we can also see that if the initial z separation between the particles approaches the particle diameter, the particles spend less time ''climbing'' over each other, and consequently the shear stress is much weaker. We thus find two necessary conditions for a positive ER effect at high shear: The dipole tilt angle must fall within an optimal range, and particles need to collide and move out of each other's

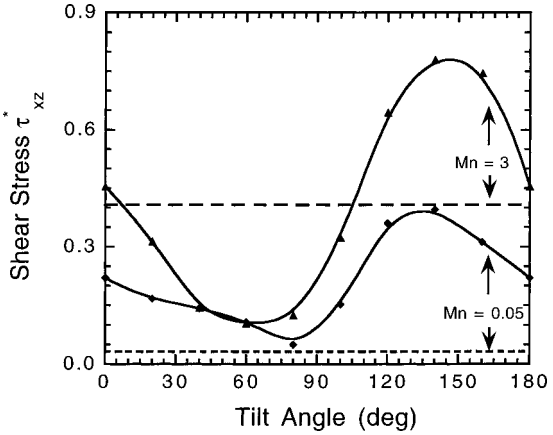

FIG. 5. Average shear stress for polydisperse particles as a function of dipole tilt angle at Mn=0.05 and 3. The dotted lines are the shear stresses without the electric forces.

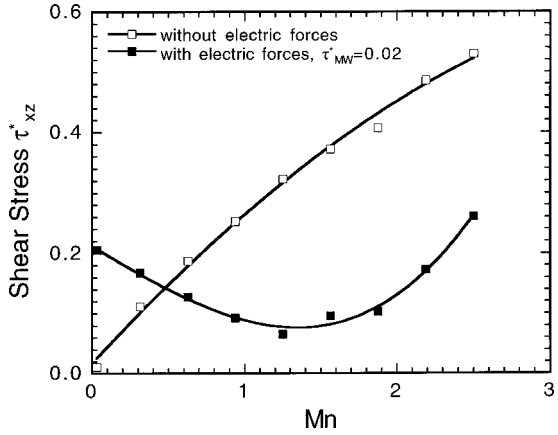

FIG. 6. Average shear stress for polydisperse particles as a function of Mason number for dielectric relaxation time $\tau^*_{MW}=0.02$. The dielectric mismatch is $\varepsilon_f/\varepsilon_p=5$, and the conductivity of the fluid σ_f is set to 0. Positive ER effects occur only for Mn$<$0.3, and negative ER effects occur only for Mn$>$0.3. The solid lines are to guide the eyes.

way. The second condition cannot be achieved if the particles have uniform sizes because the particles quickly settle into horizontal layers [27]. Consequently, we have chosen polydisperse particle sizes for our simulation. The results presented below are not sensitive to the details of the particle size distribution.

We now discuss the results of the three-dimensional simulations. Figure 5 shows the average shear stress for polydisperse particles as a function of dipole tilt angle for Mn $=0.05$ and 3. (The magnitude of the dipole moment is again set to 1.) We can see that at Mason number 0.05, positive ER effects are seen for all tilt angles. This is not surprising, because ER effects at low shear arise from the deformation of the chain structures. At Mason number 3, we can see that as in the two-particle situation, the dipole tilt angle plays a crucial role in promoting ER effects. Both positive and negative ER effects occur, depending on the tilt angle.

The next three figures examine the role of particle dielectric relaxation time. The dipole moment is calculated using Eqs. (3) and (4) with $\varepsilon_f/\varepsilon_p=5$, $\sigma_f=0$, and $\omega=0$. Figure 6 shows shear stress as a function of Mason number for τ^*_{MW} $=0.02$. These parameters give rise to tilt angles in the range of $1°-65°$ for the range of Mason numbers presented. Positive ER effects are seen only at low shear, while negative ER effects are seen only at high shear. In Figure 7, positive ER effects are seen in both the low shear and high shear regions for $\tau^*_{MW}=0.2$ (tilt angle range $8°-160°$). At Mn$\approx$0.3 (tilt angle $\sim 15°$), however, negative ER effects are seen. For $\tau^*_{MW}=2$ (tilt angle range $65°-178°$, Fig. 8), almost no ER effects appear at high shear because the magnitude of the dipole moment is significantly reduced by the particle spinning motion.

IV. DISCUSSION

To see how sensitive our simulation was to the particular details of the repulsive force we had chosen, we changed the parameter a in the repulsive force in Eq. (7) from 2 to 10. This change only resulted in a 6% increase in the stress values in Fig. 4, which seems like a reasonable indication that the general conclusions of our model are not particularly sensitive to the exact details of the repulsive force. This also suggests that if we had considered the lubrication force, which is inversely proportional to the gap distance between the particles, instead of using the somewhat artificial repulsive force of Eq. (8), we would not have changed our conclusions in any significant qualitative way.

The possible effect of mutual polarization on our results has been investigated for the simplest case of two particles approaching each other. We used only the dipole moments and assumed $\tau^*_{MW}=0$ and $\beta_0=0.5$. (Errors from using the dipole approximation become significant for $\beta_0>0.5$ [37].) Figure 9 illustrates a slight reduction in the negative ER effect when mutual particle polarization is taken into account, but this does not seem to qualitatively change our results.

The negative ER effects obtained in our simulation for

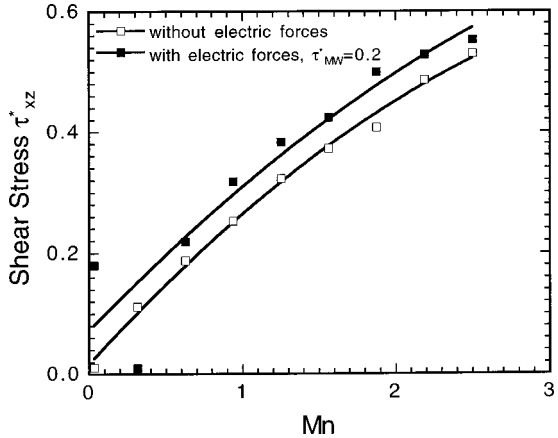

FIG. 7. Average shear stress for polydisperse particles as a function of Mason number for dielectric relaxation time $\tau^*_{MW}=0.2$. Other parameters are the same as in Fig. 6. Positive ER effects occur at both low and high shear.

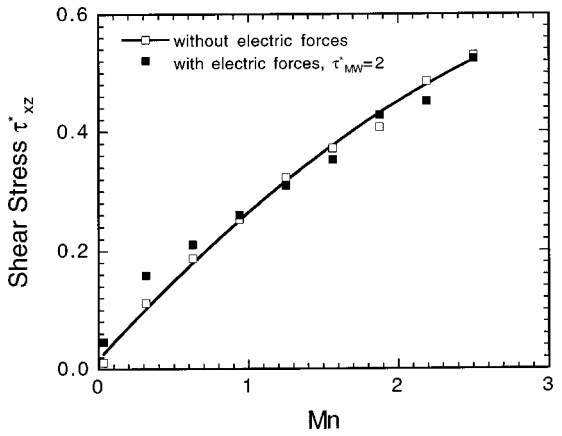

FIG. 8. Average shear stress for polydisperse particles as a function of Mason number for dielectric relaxation time $\tau^*_{MW}=2$. Other parameters are the same as in Fig. 6. There are almost no ER effects for Mn>1.

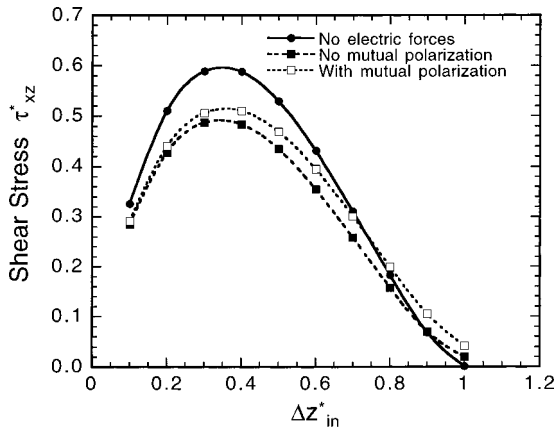

FIG. 9. Average shear stress for two identical particles colliding with each other as a function of the initial z separation between the particles, assuming Mn$=1$, $\tau^*_{MW}=0$, and $\beta_0=0.5$. The initial and final x separation is three. The solid line illustrates the case with no electric interactions; the dotted line with solid squares illustrates nonzero electric interactions without mutual polarization; and the dotted line with open squares illustrates nonzero electric interactions, including mutual polarization.

large Mason numbers also merit further discussion. In some cases, experimentally observed negative ER effects have been attributed to particle migration to one of the electrodes, causing a layer of fluid near the other electrode to be depleted of particles [38]. In other cases, however, the particle migration explanation is not convincing, because negative ER effects are observed at high shear rates, while positive ER effects are seen at low shear rates [31,32]. Our model, on the other hand, offers an explanation for why positive *and* negative ER effects can both be observed in the same system subject only to a variation in the shear rates.

By neglecting multipoles, hydrodynamic interactions, and mutual polarization between particles, our model is obviously simplified. Furthermore, since we expect multipole interactions and mutual polarization to enhance ER effects, it is not surprising that the magnitude of the shear stress obtained in our simulations falls below experimentally observed values. Nevertheless, we hope that our model will provide a starting point for future work that can incorporate more sophisticated particle-particle and particle-fluid interactions.

In summary, we have proposed a model for ER effects that takes into account the effect of FMP. At small Mason numbers, our results agree well with earlier simulation work based on the chain model. At large Mason numbers, we are able to overcome the shortcomings of the chain model and explain how ER effects can exist even when chain structures are destroyed by shear flow. We identify the tilt angle between the particle dipole moments and the applied E field as a critical parameter for ER at high shear rates. Factors affecting the tilt angle include the shear rate, particle dielectric relaxation time, and the dielectric and conductive properties of both particles and fluids. We point out that to enhance ER effects, it is necessary to adjust all of these parameters, not just one parameter alone. Finally, we can also explain why some fluids exhibit positive ER effects at low shear rates and negative ER effects at high shear rates.

ACKNOWLEDGMENTS

This work was supported by the U.S. Department of Energy (Grant No. DE-FG02-94ER45522) and by the National Science Foundation (Grant No. DMR-9971432). We thank Seth Fraden for many useful discussions. Y.H. acknowledges the support of the Brachman Hoffman Fund and of the Radcliffe Institute for Advanced Study. S.S.R.O. acknowledges the support of the Jerome A. Schiff Fund.

[1] W.M. Winslow, J. Appl. Phys. **20**, 1137 (1949).
[2] H. Block and J.P. Kelly, J. Phys. D **21**, 1661 (1988).
[3] M. Parthasarathy and D.J. Klingenberg, Mater. Sci. Eng. **17**, 57 (1996).
[4] A.P. Gast and C.F. Zukoski, Adv. Colloid Interface Sci. **30**, 153 (1989).
[5] J.E. Martin and R.A. Anderson, J. Chem. Phys. **104**, 4814 (1996).
[6] D. Adolf, T. Garino, and B. Hance, Langmuir **11**, 313 (1995).
[7] D.J. Klingenberg and C.F. Zukoski, Langmuir **6**, 15 (1990).
[8] L. C. Davis and J. M. Ginder, in *Progress in Electrorheology*, edited by K. O. Havelka and F. E. Filisko (Plenum Press, New York, 1995), p. 107.
[9] R. Tao and J.M. Sun, Phys. Rev. Lett. **67**, 398 (1991).
[10] R.T. Bonnecaze and J.F. Brady, J. Chem. Phys. **96**, 2183 (1992).
[11] F. E. Filisko, in *Progress in Electrorheology*, edited by K. O. Havelka and F. E. Filisko (Plenum Press, New York, 1995), p. 3.
[12] D.L. Klass and T.W. Martinek, J. Appl. Phys. **38**, 67 (1967).
[13] H. Uejima, Jpn. J. Appl. Phys. **11**, 319 (1972).
[14] T. B. Jones, *Electromechanics of Particles* (Cambridge Univer-

sity Press, New York, 1995), Chap. 2.
[15] P. Atten, J.-N. Foulc, and N. Felici, Int. J. Mod. Phys. B **8**, 2731 (1994).
[16] F. Ikazaki, A. Kawai, K. Uchida, T. Kawakami, K. Edamura, K. Sakurai, H. Anzai, and Y. Asako, J. Phys. D **31**, 336 (1998).
[17] K. O. Havelka, in *Progress in Electrorheology*, edited by K. O. Havelka and F. E. Filisko (Plenum Press, New York, 1995), p. 43.
[18] J. Hemp, Proc. R. Soc. London, Ser. A **434**, 297 (1991).
[19] H. Block, K.M.W. Goodwin, E.M. Gregson, and S.M. Walker, Nature (London) **275**, 632 (1978).
[20] H. Block, J.P. Kelly, A. Qin, and T. Watson, Langmuir **6**, 6 (1990).
[21] H. Block, E. Kluk, J. McConnell, and B.K.P. Scaife, J. Colloid Interface Sci. **101**, 320 (1984).
[22] Y. Hu, J. Lee, and T. Bao, in *Proceedings of the Sixth International Conference on Electrorheological Fluids, Magnetorheological Suspensions and Their Applications*, edited by M. Nakano and K. Koyama (World Scientific, Singapore, 1998), p. 123.
[23] J.T.K. Wan, K.W. Yu, and G.Q. Gu, Phys. Rev. E **62**, 6846 (2000).
[24] H. Block and P. Rattray, in *Progress in Electrorheology*, edited by K. O. Havelka and F. E. Filisko (Plenum Press, New York, 1995), p. 19.
[25] K. Negita and Y. Ohsawa, Phys. Rev. E **52**, 1934 (1995).
[26] D.J. Klingenberg, F. van Swol, and C.F. Zukoski, J. Chem. Phys. **94**, 6160 (1991).
[27] J.R. Melrose, Mol. Phys. **76**, 635 (1992).
[28] M. Whittle, J. Non-Newtonian Fluid Mech. **37**, 233 (1990).
[29] H. See and M. Doi, J. Rheol. **36**, 1143 (1992).
[30] D.J. Klingenberg, F. van Swol, and C.F. Zukoski, J. Chem. Phys. **94**, 6170 (1991).
[31] A. W. Schubring and F. E. Filisko, in *Progress in Electrorheology*, edited by K. O. Havelka and F. E. Filisko (Plenum Press, New York, 1995), p. 215.
[32] J. Trlica, O. Quadrat, P. Bradna, V. Pavlínek, and P. Sáha, J. Rheol. **40**, 943 (1996).
[33] It can be shown that the particle surface conductivity contributes to an effective particle bulk conductivity. See, for example, G. Schwarz, J. Phys. Chem. **66**, 2636 (1962).
[34] M. Doi and S. F. Edwards, *The Theory of Polymer Dynamics* (Oxford University Press, London, 1986).
[35] Yue Hu, Ee-Yenn E. Lin, and Ujitha M. Dassanayake, in *Proceedings of the Eighth International Conference on Electrorheological Fluids and Magnetorheological Suspensions*, edited by G. Bossis (World Scientific, Singapore, 2002), p. 640. We have seen no qualitative difference between two-and three-dimensional results.
[36] K. Tanaka, K. Ichizawa, Y. Onishi, A. Kubono, and R. Akiyama, in *Proceedings of Eighth International Conference on Electrorheological Fluids and Magnetorheological Suspensions* [Ref. [35]), p.773.
[37] T. B. Jones, *Electromechanics of Particles* (Cambridge University Press, New York, 1995), Sec. 6.3.
[38] C.W. Wu and H. Conrad, J. Rheol. **41**, 267 (1997).